IOPscience iopscience.iop.org

Home Search Collections Journals About Contact us My IOPscience

Alkanethiol headgroup on metal (111)-surfaces: general features of the adsorption onto group 10 and 11 transition metals

This article has been downloaded from IOPscience. Please scroll down to see the full text article.

2007 J. Phys.: Condens. Matter 19 176004

(http://iopscience.iop.org/0953-8984/19/17/176004)

View the table of contents for this issue, or go to the journal homepage for more

Download details:
IP Address: 129.252.86.83
The article was downloaded on 28/05/2010 at 17:53

Please note that terms and conditions apply.

IOP PUBLISHING JOURNAL OF PHYSICS: CONDENSED MATTER

J. Phys.: Condens. Matter **19** (2007) 176004 (11pp) doi:10.1088/0953-8984/19/17/176004

Alkanethiol headgroup on metal (111)-surfaces: general features of the adsorption onto group 10 and 11 transition metals

Luca M Ghiringhelli, Riccarda Caputo and Luigi Delle Site

Max Planck Institute for Polymer Research, Ackermannweg 10, 55128 Mainz, Germany

E-mail: ghiluca@mpip-mainz.mpg.de and dellsite@mpip-mainz.mpg.de

Received 15 January 2007, in final form 21 February 2007
Published 3 April 2007
Online at stacks.iop.org/JPhysCM/19/176004

Abstract

Using first-principles density-functional calculations, we studied the adsorption of methylthiolate (CH_3S) on (111)-surfaces of the transition metals belonging to group 10 (Ni, Pd, and Pt), and two group 11 metals, Ag and Au. By making a systematic comparison between the different metals, we identify general adsorption properties and clarify them in terms of the interplay between energies, structures and electronic details. On the basis of electron density arguments, we suggest an explanation for the preference of the face-centred cubic (fcc) above the hexagonal close-packed (hcp) hollow site for the adsorption onto (111) metal surfaces. In nanotechnological applications, our analysis may serve to rationalize the optimal choice of the substrate when a given property is required.

(Some figures in this article are in colour only in the electronic version)

1. Introduction

The pioneering work of Nuzzo and Allara [1], on experimental techniques for preparing supported oriented monolayers of polyfunctional organic molecules with a variety of molecular structures, has opened a new and very broad area of research. Nowadays the term self-assembly monolayers (SAMs) is widely used to describe those systems where molecules spontaneously form ordered molecular assemblies. In this context, thiol-based SAMs are routinely used to provide the anchoring site of the molecule onto the surface, and they turn out to be the driving element in the self-assembly process. For this reason, the adsorption on metal surfaces of functionalized long-chain molecules, such as alkanethiols, has become of great importance for designing self-assembled monolayers. Because of their wide variety of functions, their application spans from material science to biophysics [2–8]. The structural characteristics of alkanethiol monolayers self-assembled on metal substrates derived from different experimental measurements [9–11, 2, 12, 5, 13, 14] point to a decisive role played

by the substrate/headgroup interactions in the equilibrium structure formation. The possibility to control the geometry and the molecular arrangement on the surface makes the studies of organic molecular SAMs a very important and attractive research field (see, e.g. [15, 7, 16] and references therein). Generally the nature of the substrate/headgroup bond can vary from covalent to polar [4, 17, 18], but, as reported in [4, 16], the reaction mechanism is still not well understood. It is generally accepted that thiol-based self-assembly on gold occurs through an electrochemical reaction at the interface between the molecule and the metal substrate. In addition, little is known about their general structural and electronic properties for different substrates. This aspect represents a crucial point for designing and optimizing SAM structures with specific properties on demand. Some early works [5, 2, 3] partially addressed the question of how the structure of the monolayers is influenced by the choice of the metal substrate. The answer to the question whether there is a trend in the adsorption properties for different metals with similar characteristics, such as the transition metals, may definitely help in understanding the adsorption process. Here we present a systematic density-functional study of the structural and energetic properties of CH_3S adsorbed on the transition metals of group 10, namely Ni, Pd, Pt and two metals of group 11, namely Ag and Au. Descending group 10, we considered elements with 3d (Ni), 4d (Pd), and 5d (Pt) valence orbitals, and in group 11, we studied elements with 4d (Ag) and 5d (Au) valence orbitals. The comparative study we present here proceeds in different directions. The adsorption onto three metal surfaces (Pt, Ag, and Au) has been carried out at three different coverages, namely 1/3 (i.e. the full coverage; see e.g. [5, 19, 20]), 1/4, and 1/9 monolayer (ML). At all these coverages, the trends along the minimal series Ag–Au, descending group 11, and Pt–Au, moving along the 5d period, can be followed. Only for the intermediate coverage are the series Ni–Pd–Pt, descending the group 10, and the series Pd–Ag, along the 4d period, studied and discussed. The two series along the period (Pd–Ag and Pt–Au) are actually represented by only two elements each; nonetheless, by moving from almost filled to completely filled d-band metals, we intentionally focus on the maximum expected change between adjacent elements along the period. Au, Ag, and Pt are selected for the thorough study at different coverages due to their technological and experimental greater relevance, when compared to Ni and Pd, in SAM applications. We focused on the interplay between the strength of the molecule–surface bond and the structural properties upon adsorption for the different metals considered. We aim to clarify central open questions such as the nature of the optimal adsorption sites and substrate-dependent properties, and address the problem of the coverage dependence.

Here we stress that we do not consider the formation of possible over-structures of the adsorbates, since we restrict ourselves to the electronic properties of one adsorbed molecule per unit cell. This is because the problem under examination is inherently multi-scale in its nature, where mainly electronic features (the adsorption of the single molecule) and mainly statistical features (the formation of over-structures) can be decoupled. Our study has thus a double purpose: (a) to suggest to the SAM experimentalist or engineer a rational way to choose the optimal substrate when a certain property is required, and (b) to serve as a basis for a classical, multi-scale, modelling of the CH_3S–metal surface interaction, as has already been successfully done in [21], where CH_3S is considered as the headgroup of longer-chain alkanethiols.

2. Computational details

We use the density-functional-based finite-electronic temperature method (FEMD) [22] implemented in the plane-wave-based CPMD code [23]. In this method the electron density and the Hellman–Feynman forces are determined via a subspace diagonalization of the high-

temperature electron density matrix. The subspace is expanded in a plane-wave basis set that in our set-up is cutoff at 60 Ryd, a value which turned out to be sufficient after some tests at higher cutoff values up to 90 Ryd. We employed norm-conserving-type pseudopotentials, generated according to Troullier–Martins scheme, except for sulfur, where we made use of a Goedecker-type pseudopotential; all the pseudopotentials were accurately tested against bulk and surface properties for the metals, and correct structural properties for the molecule. We use the (spin-restricted) Perdew–Burke–Ernzerhof (PBE) [24] generalized gradient corrected functional. The prototype system consists of a (111) surface represented by four layers separated by four layers of vacuum. We employ supercells of different sizes: 2×2 unit cell for all metals and also $(\sqrt{3} \times \sqrt{3})$R30° and 3×3 unit cells for Pt, Ag, and Au. Since our systems consist of only one, periodically replicated, adsorbed molecule, the different cell sizes are employed to mimic different coverages. In particular, one adsorbed CH_3S per $(\sqrt{3} \times \sqrt{3})$R30° supercell represents coverage of 1/3 ML (a value that matches the experimentally found full coverage), one CH_3S per 2×2 supercell and one CH_3S per 3×3 represent coverage of 1/4 and 1/9 ML, respectively. We use a $6 \times 6 \times 1$ k-point mesh in the Monkhorst–Pack scheme, for the smaller and intermediate cell, and a $4 \times 4 \times 1$ mesh for the larger cell. This set-up for the k-point mesh turned out to be optimal, after extended tests were carried on using finer and coarser mesh sizes. Unconstrained geometry optimizations were carried out using the BFGS algorithm; we considered our structures to have converged whenever the maximum components of all the forces were below 2×10^{-3} atomic units and the total energies changed by less than 10^{-4} Hartree across two subsequent optimization steps. With our setting, we estimate an overall accuracy of 0.05 eV on our adsorption energies.

3. Results

3.1. Energy and geometry

Table 1 reports adsorption energies and geometric details of the adsorption of methylthiolate (CH_3S) onto the different surfaces. For each metal and coverage, initial configurations were prepared with the molecule above the four high-symmetry sites for the (111) surface. The surface and the molecule were previously optimized in separate supercells. The axis of the molecule was prepared vertical with the sulfur atom at 2.00 Å above the site[1]. Relaxation of all the atoms of the surface and the molecule led to the final configuration that is recorded in table 1.

The adsorption energy per CH_3S molecule adsorbed on the metal surface is given by

$$E_{\text{ads}} = E_{\text{tot}}(\text{CH}_3\text{S(Me)}) - E_{\text{tot}}(\text{Me}) - E_{\text{tot}}(\text{CH}_3\text{S}) \tag{1}$$

where $E_{\text{tot}}(\text{CH}_3\text{S(Me)})$, $E_{\text{tot}}(\text{Me})$, $E_{\text{tot}}(\text{CH}_3\text{S})$ are the total energies of the adsorbed system, the clean surface and the gas-phase molecule respectively.

Although it is more typical to fix some of the bottom layers of the metal and let only two or three topmost layers relax, we let all the metal atoms relax. Some tests with fixed layers revealed negligible difference in adsorption energy with the fully unconstrained optimization. The four layers relax in the system without the molecule and, when the molecule is placed in the box and adsorbed, only the two topmost layers interact with the molecule. This is seen by looking at the negligible displacement of the two bottom layers, but also more clearly with the electron density difference maps we show in figures 1–3.

[1] When we considered adsorption on the atop site, where the equilibrium distance is longer than 2.00 Å on all our substrates, we also tried with initial distances of 2.5 Å, whenever we could not find a local minimum starting from 2.00 Å.

Table 1. Adsorption energies and structural data for the stable geometries of CH_3S adsorbed on the (111) surface of Ni, Pd, Pt, Ag, and Au. Pt, Ag, and Au were considered at three different coverages: 1/3 ML (i.e. one CH_3S per $(\sqrt{3}\times\sqrt{3})$R30° metal surface cell), 1/4 ML (one CH_3S per 2×2 metal surface cell), and 1/9 ML (one CH_3S per 3×3 metal surface cell). For Ni and Pd only the intermediate coverage was treated. Adsorption energies (E_{ads}) are given in eV. We use 'unstable' when either the molecule was repelled from the surface or the molecule moved to another symmetry site. Highlighted are the adsorption energies of the most stable adsorption sites, for each metal (Me) and coverage. All distances are in Å and angles in degree. Below the name of the metal atoms, we report the equilibrium distance between neighbours in the ideal lattice, as given by our settings. The height of the sulfur atom above the surface (h_S) is calculated as $h_S = z_S - \bar{z}_{Me}$, where z_S is the z-coordinate of the S atom and $\bar{z}_{Me}$ is the average z-coordinate of the top layer of the metal. The quantity d_{S-Me} is the distance between the sulfur atom and the *closest* metal atom. The tilt angle with respect to the vertical to the plane is calculated as $\arccos((z_C - z_S)/d_{S-C})$, where z_C is the z-coordinate of the C atom and d_{S-C} is the distance between the sulfur and carbon atoms. For tilt angles larger than 2°, we specify between brackets the first letter of the site towards which the axis of the adsorbed molecule bends. The displacement δ_{Site} indicates the distance between the projection onto the surface plane of sulfur atom's position and the position of the closest ideal symmetry site. The ideal site position is defined with respect to the actual position of the surface atoms. Thus, the ideal site position is the position of one atom for the atop site, the centre of mass of two or three atoms for the bridge and hollow sites, respectively. For displacements larger than 0.05 Å, the first letter of the site towards which the adsorbed molecule is displaced is specified between brackets.

Me	Site	E_{ads}	h_{S-Me}	d_{S-Me}	α	δ_{Site}
				1/3 ML		
Pt	Atop			Unstable		
(2.82 Å)	Bridge	−1.87	1.85	2.32	0.8	0.05
	fcc	**−2.42**	1.52	2.30	1.4	0.01
	hcp	−2.27	1.62	2.30	0.6	0.03
Ag	Atop	−1.03	2.19	2.40	0.4	0.01
(2.93 Å)	Bridge	−1.71	1.95	2.52	0.6	0.03
	fcc	**−1.87**	1.84	2.57	0.2	0.00
	hcp	−1.83	1.89	2.58	0.1	0.01
Au	Atop			Unstable		
(2.92 Å)	Bridge	−1.29	1.96	2.53	0.8	0.04
	fcc	**−1.54**	1.75	2.53	0.5	0.02
	hcp	−1.43	1.92	2.61	0.0	0.00
				1/4 ML		
Ni	Atop	−1.59	2.03	2.13	1.7	0.05
(2.53 Å)	Bridge	−2.74	1.58	2.13	6.1 (f)	0.23 (h)
	fcc	**−2.93**[a]	1.59	2.12	9.3 (b)	0.03 (f)
	hcp	−2.92	1.60	2.17	9.6 (t)	0.02
Pd	Atop			Unstable		
(2.81 Å)	Bridge			Unstable		
	fcc	**−2.73**	1.58	2.27	9.8 (b)	0.04
	hcp	−2.70	1.60	2.28	10.4 (t)	0.02 (f)
Pt	Atop			Unstable		
(2.82 Å)	Bridge			Unstable		
	fcc	**−2.67**	1.55	2.25	11.7 (t)	0.04
	hcp	−2.45	1.65	2.28	22.5 (t)	0.05
Ag	Atop	−1.05	2.31	2.42	1.7	0.07 (b)
(2.93 Å)	Bridge			Unstable		
	fcc	**−1.88**	1.92	2.54	10.6 (b)	0.04
	hcp	−1.87	1.93	2.56	21.4 (t)	0.09 (b)

Table 1. (Continued.)

Me	Site	E_{ads}	h_{S-Me}	d_{S-Me}	α	δ_{Site}
				1/4 ML		
Au	Atop			Unstable		
(2.92 Å)	Bridge	−1.46	2.23	2.40	35.0 (t)	0.38 (t)
	fcc	−1.51	1.88	2.52	12.8 (b)	0.01
	hcp	**−1.53**[b]	1.96	2.51	21.2 (b)	0.09 (b)
				1/9 ML		
Pt	Atop			Unstable		
(2.82 Å)	Bridge			Unstable		
	fcc	**−3.01**	1.49	2.26	10.4 (t)	0.03
	hcp	−2.68	1.58	2.28	13.0 (b)	0.07 (b)
Ag	Atop			Unstable		
(2.93 Å)	Bridge			Unstable		
	fcc	**−1.94**	1.87	2.51	22.4 (t)	0.08 (b)
	hcp	−1.90	1.89	2.53	11.8 (b)	0.05
Au	Atop	−0.79	2.29	2.39	9.0 (b)	0.50 (b)
(2.92 Å)	Bridge	−1.51	1.77	2.43	3.5 (t)	0.20 (h)
	fcc	**−1.76**	1.71	2.48	0.9	0.02
	hcp	−1.67	1.75	2.49	0.9	0.02

[a] Compare to [3]: using many-electron embedding theory, they found no energy difference between the fcc and the hcp hollow sites, for the adsorption of CH_3S onto the Ni(111) of a 62-atom Ni *cluster*. The adsorption energy they report is −2.64(hollow), −2.43(bridge), −1.95(atop) eV.
[b] Compare to [29]: they found, as the most adsorbing site of CH_3S onto Au(111) at the coverage of 1/4 ML, an hcp-bridge site with $E_{ads} = -1.72$ eV (with the PW91 functional) or −1.25 eV (with the RPBE functional).

In several cases we observed local minima that are not reported in table 1: we preferred to limit ourselves to the most adsorbing state per site (for every site where adsorption occurred). Those other minima displayed, with respect to those we report, a different displacement from the perfect site and different tilt angles. In agreement with the findings of [25, 26], this suggests that the adsorption energy landscape is rather complicated on these metals. This property, combined with the four initial conditions per metal per coverage, leads to a thorough spanning of the configurational space for the cases studied. The robustness of our analysis, that is oriented towards the study of trends, is witnessed by the equality of initial condition for the geometry optimization procedures.

In the following we analyse the features of the different adsorptions, as emerging from their energetic and geometric properties. We will in particular insist on any trend that can be evidenced, along the different directions already mentioned in the introduction.

3.1.1. Adsorption energy. Looking at table 1, the trend in adsorption energy is evident: it decreases (in absolute value) in descending the group and moving to the right along the period. This is consistent with [27], where the adsorption of CH_3S along group 11 (Cu, Ag and Au) was studied[2]. The calculated values of the adsorption energy for methanethiolate adsorbed on Au surface, available in the literature, ranges from −1.67 eV [28] (at coverage 1/3 ML) to −1.69 eV (at coverage 1/9 ML), and −1.72 eV [29] (at coverage 1/4 ML; in the same reference the value −1.43 eV is also indicated, if the RPBE functional is used rather than

[2] Our observed trend also compares well with reference [26], when high coverage is considered. The low-coverage limit in [26] is studied on an isolated cluster consisting of two metal layers and those not straightforwardly comparable with our setting.

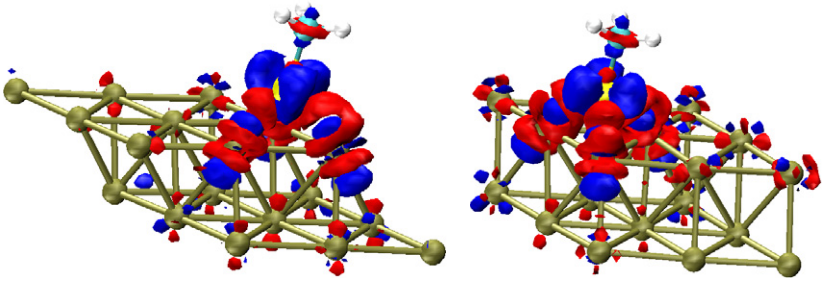

Figure 1. Perspective view for the adsorption of CH_3S onto Pt(111). Regions of positive (red/light grey) and negative (blue/dark grey) electron density displacement are displayed by iso-surfaces at the value $\pm 0.027\ e\ \text{Å}^{-3}$. Left: hcp-hollow site. Right: fcc-hollow site. Only the upper two of the four layers used in the simulation are shown.

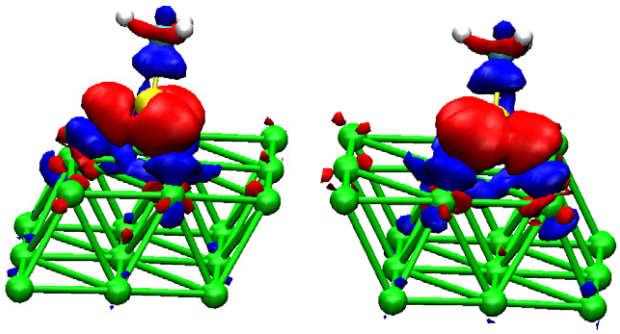

Figure 2. Perspective view for the adsorption of CH_3S onto Ag(111). Regions of positive (red/light grey) and negative (blue/dark grey) electron density displacement are displayed by iso-surfaces at the value $\pm 0.011\ e\ \text{Å}^{-3}$. Left: hcp-hollow site. Right: fcc-hollow site. Only the upper two of the four layers used in the simulation are shown.

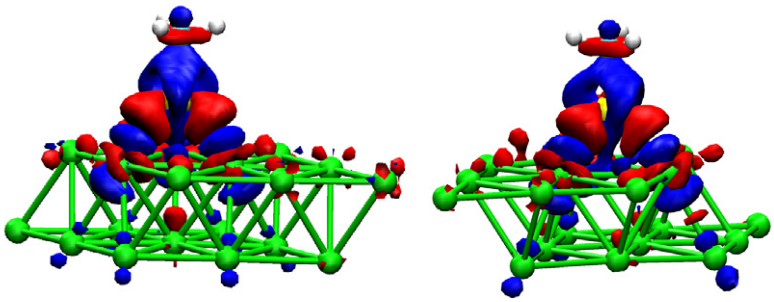

Figure 3. Perspective view for the adsorption of CH_3S onto Au(111). Regions of positive (red/light grey) and negative (blue/dark grey) electron density displacement are displayed by iso-surfaces at the value $\pm 0.011\ e\ \text{Å}^{-3}$. Left: hcp-hollow site. Right: fcc-hollow site. Only the upper two of the four layers used in the simulation are shown.

the PW91), whilst the experimental value reported is -1.73 eV [16] for coverages lower than 1/4 ML. Our calculated value at coverage 1/9 ML is -1.76 eV. Some early calculations [3] using many-electron embedding theory on the chemisorption of CH_3S on the Ni(111) surface

found no adsorption energy difference between hollow sites (both fcc and hcp sites) and the bridge site on which, as also reported in [12], the adsorption energy is equal to −2.64 eV.

In general, we find that adsorption energies increase in magnitude with decreasing coverage. The difference in adsorption energies at different coverages is almost negligible for Ag. For Au the adsorption energy trend with coverage differs from site to site, though the adsorption energies changes are within 0.24 eV passing from full to 1/9 ML coverage. For Pt the difference is rather consistent, changing by more than 0.5 eV from the highest to the lowest coverage.

3.1.2. Adsorption sites. According to table 1, for all metals the energetically most favoured adsorption site is always the three-fold hollow-fcc site, regardless of the coverage[3]. The only exception appears to be Au at intermediate coverage, but there the difference in adsorption energy between the two hollow sites is lower than our overall accuracy. The most stable configuration as a function of the coverage is still a controversial open question not only for the Au substrate [7, 11, 19, 30, 31, 27, 32, 5, 20] which has been widely studied, but also for other substrates, which have been by far less investigated. In [25, 31] it is claimed that *'coverage does not affect site preference'*, and that for coverages 1/12, 1/4, 1/3 ML[4] the thiol molecules adsorb on the Au(111) surface on the fcc site, independently also of the chain length. We can confirm these statements, at least for what concerns the headgroup behaviour.

We find that the higher the coverage, the higher is the number of stable adsorption sites available for Ag and Pt. For Au, bridge and hollow sites are stable adsorption sites at all coverages, while, curiously, the top site is stable only at low coverage. Actually, the adsorption site that is labelled 'atop' for Au at 1/9 ML is the most off-centred adsorption site we found, being displaced towards the bridge site, at 34% of the atop–bridge distance.

3.1.3. Adsorption distances and tilt angles. We define the adsorption distance as $h_{\mathrm{S-Me}} = z_{\mathrm{S}} - \bar{z}_{\mathrm{Me}}$, where z_{S} is the z-coordinate of the S atom and $\bar{z}_{\mathrm{Me}}$ is the average z-coordinate of the top layer of the metal. Looking at the adsorption onto the fcc and hcp sites, $h_{\mathrm{S-Me}}$ stays almost constant along the group, while it increases noticeably moving to the right in the periodic table (thus looking at the pairs Pt–Au and Pd–Ag).

Looking at the distance ($d_{\mathrm{S-Me}}$) of closest approach between sulfur and atoms of the metal surface, one can note a difference between group 10 and 11 metals. In group 10, each metal displays a peculiar $d_{\mathrm{S-Me}}$, that stays rather constant upon changing adsorption site (and, in the case of Pt, also changing coverage). In group 11, $d_{\mathrm{S-Me}}$ is more variable; it is the shortest for atop adsorptions, intermediate for bridge, and the longest for hollow adsorptions. The difference between the shortest and the longest distance in $d_{\mathrm{S-Me}}$ goes up to 0.2 Å, for Ag, and up to 0.1 Å for Au.

Whenever the molecule adsorbs to an atop site, one can note that the height of sulfur above the average surface (h_{S}) is shorter than the shortest distance to a metal atom. This apparent incongruence has two different motivations. For the two atop adsorptions at intermediate coverage (Ni and Ag) and the atop adsorption onto Pt at full coverage, the surface is markedly distorted by the adsorption; in fact, the metal atom in the atop position 'sinks', having its z-coordinate lowered by more than 0.1 Å with respect to the average position of the rest of the surface. In contrast, at low coverage the only atop binding we found was on Au(111). As we

[3] This is consistent with reference [26], albeit our measured displacements from the perfect (fcc) site have always smaller magnitude than in [26].

[4] We have converted the coverages of references [25, 31] into our notation; in the original papers coverage 1 is defined as one adsorbed molecule per $(\sqrt{3} \times \sqrt{3})$R30 surface unit cell, i.e. comprising three atoms. Thus, the conversion from references [25, 31] into ours is simply performed by dividing by those three values.

have already pointed out before, that adsorption is located at a quite off-centred position with respect to the atop site (0.50 Å, i.e. 34% displaced towards a bridge site), thus easily accounting for $h_S < d_{S-Me}$.

The tilt angle assumes a large range of values, from 0 to 35°, with no detectable systematic behaviour at intermediate and low coverage. At full coverage, the bending angle is always negligible for all the adsorptions we found. It has to be said that the molecule always bends in order to have two hydrogen atoms pointing towards the surface, rather than only one.

Given that the equilibrium distance for the S–C bond for the isolated molecule is 1.78 Å, for an adsorbed molecule this distance always increases to a value between 1.82 and 1.85 Å. Whenever the molecule adsorbs on the atop site, the elongation of the C–S bond is always shorter (1.82 Å) than for adsorption onto the two-fold and three-fold sites. The elongation is reflected in an accumulation of electron density, that can be seen in the density maps, in the region along the C–S bond (see below).

We calculated for each adsorption the displacement (δ_{Site}) from the perfect symmetry site. The displacement is referred to the actual optimized position of the one, two, and three atoms defining the atop, bridge, and hollow sites, respectively. For adsorption in the full coverage regime, the displacement from the perfect site is always very small (<0.05 Å). At intermediate and low coverage, when the molecule is adsorbed onto a hollow site, the displacement from the perfect site is small (<0.1 Å). Larger displacements are only seen in correspondence to adsorptions onto the atop or bridge sites.

The adsorption distance (h_S) shows a maximum at intermediate coverage, being smaller at full and low coverage. In contrast, the minimum distance between sulfur and a surface atom (d_{S-Me}) tends to increase with increasing coverage. Note that the displacement from the perfect symmetry site (δ_{Site}), together with the independent relaxation of the surface atoms, easily accounts for the apparent discrepancy in trend for the two distances.

3.2. Electronic properties

3.2.1. Electron density displacement maps. We analyse the electronic properties of the systems, through the electron density displacement, $\Delta\rho(\boldsymbol{r})$. This quantity is calculated by subtracting from the electron density of the adsorbed system the densities of the isolated CH_3S and of the surface. In figures 1–3 we show selected adsorption geometries with positive and negative iso-surfaces of the electron density displacement. All the selected geometries refer to the 3×3 supercell and both hollow adsorption sites for the three metals (Pt, Ag, and Au) studied at this coverage. Note that for Ag and Au we chose the same iso-surface value (0.011 e Å^{-3}), while for Pt this value is 2.5 times (0.027 e Å^{-3}) larger than for the other group 11 metals. The justification for this choice is given at the end of the section, when an integral quantity related to the electron density displacement is introduced. From the observation of the electron density displacement maps, several features become evident. In the following we describe them.

In all cases, only the sulfur atom of the molecule interacts directly with the surface. By this we mean that the electron density displacement s induced on the sulfur atom is mirrored by opposite sign displacements on the surface, whereas a similar correspondence is not visible for the electron density displacement induced on the methyl group. In the cases displayed, all hollow site adsorptions, three atoms of the first layers are interested in a chemical bond with the sulfur atom. The chemical bond between sulfur and the surface is characterized, following the line joining the involved nuclei, by the alternation of electron density accumulation, on the sulfur side, and electron density depletion on the surface side. This is consistent with a similar analysis reported in [28], for the adsorption onto Au(111) at a bridge site. The molecule is

interested in a moderate internal charge redistribution, that is reflected in the elongation of the C–S bond with respect to the gas-phase molecule.

For all the three metals, upon adsorbing onto a fcc site, the electron density displacement propagates to the second topmost layer, along the three bonds between S and the three topmost layer atoms. The bond is identified by accumulation (midway) and depletion (around the atom) of electron density. This gives the suggestive picture of the sulfur atom anchored like a tripod to two metal layers. The three atoms of the second layer, that can be seen as the vertices of a triangle staggered with the triangle whose vertices are the three atoms surrounding the fcc site, are affected by a small electron density accumulation (this feature is not visible for Ag at the iso-surface level we chose).

For the three metals as well, upon adsorbing onto an hcp site, the three bonding atoms of the topmost layer each have three neighbours in the lower layer, none of which is aligned with the S–Me bond. One of these three second layer neighbours is shared and corresponds to an atom in an atop position with respect to the sulfur atom. The other two neighbours per surface bonded atom arrange in a hexagon centred around the shared neighbour. The bonding is propagated in the second layer to the six other than the central neighbours with an electron density depletion around the six atoms and an electron density accumulation in a position corresponding to the barycentres of the three equilateral triangles defined by each topmost bonded metal atom and their two non-shared neighbours (this last electron density accumulation is not visible at the iso-surface level we chose). On the other hand, the shared neighbour in the second layer displays an electron density accumulation in its surroundings, that has to be regarded as an anti-bonding signal.

On a closer look, the two 5d metals share a characteristic contrasting with Ag, the 4d metal. For Pt and Au, the three electron density accumulation clouds surrounding the sulfur atom are separated by electron density depletion regions, while for Ag those regions are connected. In other words, for Ag, one can draw a closed path around Ag (e.g., a circumference in a horizontal plane containing the sulfur nucleus), touching points in which the electron density displacement is always positive, while for Au and Pt, one would encounter six zeros on such a closed path. This holds for the adsorption in both hollow sites.

We note that only the two topmost layers are significantly affected by the electron density displacement, at least at the iso-surface level chosen for display. The most penetrating bonding is, predictably, the bonding onto Pt, where some charge redistribution is visible for values around 0.01 e Å^{-3} at the third layer (not shown in the figures).

The above-mentioned observations also suggest that a 3×3 supercell can be regarded as an (almost) isolated case for the adsorption. At the distance of the periodic replicas of the molecules (around 9 Å) there must be negligible intermolecular interaction; furthermore, figures 1–3 suggest that, in the second topmost layer, the atoms affected by the electron density displacement are contained either in a equilateral triangle of edge two metallic bond lengths (adsorption on the fcc site) or in a hexagon of side one bond length (on the hcp site). These regions are fully contained in a 3×3 supercell but *not* in a 2×2, where atoms of the second layers would be shared by adjacent electron density displacement regions yielding a rather complicated electron density displacement pattern. At the topmost layer, the three atoms that are closest neighbours to the hollow site are obviously those displaying larger electron density displacement. On the other hand, all the nine surface atoms appear to be interested in some electron density displacement. Close inspection of the orientation of the polarization clouds suggests that a small amount of electron density displacement is shared among periodic images for the six atoms that do not neighbour the adsorption site. All these considerations suggest that the change in adsorption energy on going to coverage lower than 1/9 ML would be very small. This observation is most critical for the case of Pt, where the surface atoms are evidently

more polarized. That is the case is which we expect the bigger change in adsorption energy on going to a lower coverage.

3.2.2. Total number of transferred electrons. We define the number of transferred electrons as

$$Q = \tfrac{1}{2} \int \mathrm{d}\boldsymbol{r}\ |\Delta\rho(\boldsymbol{r})| \tag{2}$$

where the integration domain is the complete supercell. For Pt, we find $Q = 1.44\ e$ (fcc) and $Q = 1.45\ e$ (hcp). For Ag we find $Q = 0.55\ e$ (fcc) and $Q = 0.56\ e$ (hcp). For Au we find $Q = 0.69\ e$ (fcc) and $Q = 0.68\ e$ (hcp). The number of transferred electrons is always almost the same in the two hollow sites for the same metal. Thus, the three-fold anchoring of the fcc site is (geometrically) more 'efficient' a bonding than the six-fold propagation of the hcp site. The much higher Q value for Pt, with respect to the group 11 metals, explains the need for the choice of different iso-surface values in figures 1–3. In fact, the different values were required by the need of display clarity. A high value for the group 11 metals would have almost led to the disappearance of the displayed electron density displacement, while a low value for Pt would have caused the electron density displacement clouds to almost fill the space.

4. Conclusions

We have reported a density-functional study of the adsorption of methylthiolate onto (111) surfaces of group 10 metals (Ni, Pd, and Pt) and group 11 metals (Ag and Au). Three of these metal surfaces were studied at three different coverages: 1/3, 1/4, and 1/9 ML. The highest coverage corresponds to the experimentally observed full coverage of alkanethiols on Au(111). We provide electron-density-based arguments to support the thesis that at 1/9 ML the adsorption can be considered as close to the isolated case (i.e. adsorption energies and geometries might not change dramatically on further decreasing the coverage).

We find that the energetically most favoured adsorption sites is always the fcc-hollow site, for all metals and all coverages (an exception being gold at 1/4 ML, where the most favoured site is the hcp hollow, albeit with almost the same adsorption energy as the fcc hollow). We find that adsorption energies decrease in magnitude descending the group (i.e. adding an electron shell each step) and moving to the right along the period (i.e., in our case, filling the d-band). Adsorption energies increase in magnitude upon decreasing coverage.

We analysed the sulfur–metal chemical bonds for the adsorption onto the hollow sites of Au, Ag, and Pt, by means of electron-density displacement maps. On the basis of those maps, we provide an argument for the justification of the difference in adsorption energies between the two hollow sites, a difference that can be found in all metals we studied.

Our systematic study of the adsorption of the methanethiolate onto different substrates, together with the analysis of energetic and geometrical properties of the adsorption, may be used for a rational choice of the surface for adsorption experiments and engineering applications based on self-assembly-monolayer (SAM) formation on metallic surfaces, when specific properties are required to be optimized on demand. Furthermore, our data already served as a basis for a multi-scale modelling [21] of SAM systems, allowing for large-scale simulations with longer-chain alkanethiols, in order to search for statistical properties of the systems.

Acknowledgments

We thank K Kremer for valuable suggestions. We thank D Sebastiani and S Iacopini for a critical reading of the manuscript. LDS acknowledges the support of the Volkswagen Foundation.

References

[1] Nuzzo R G and Allara D L 1983 *J. Am. Chem. Soc.* **105** 4481
[2] Lee T R, Laibinis P E, Folkers J P and Whitesides M 1991 *Pure Appl. Chem.* **63** 821
[3] Yang H, Caves T C, Whitten J L and Huntley D R 1994 *J. Am. Chem. Soc.* **116** 8200
[4] Sellers H, Ulman A, Shnidman Y and Eilers J E 1993 *J. Am. Chem. Soc.* **115** 9389
[5] Fenter P, Eisenberger P, Li J, Camillone N, Bernasek S, Scoles G, Ramanarayanan T A and Liang K S 1991 *Langmuir* **7** 2013
[6] Swalen J D, Allara D L, Andrade J D, Chandross E A and Garoff S 1987 *Langmuir* **3** 932
[7] Schreiber F 2004 *J. Phys.: Condens. Matter* **16** R881
[8] Love J C, Estroff L A, Kriebel J K, Nuzzo R G and Whitesides G M 2005 *Chem. Rev.* **105** 1103
[9] Lee J G, Lee J and Yates J T Jr 2004 *J. Phys. Chem.* B **108** 1686
[10] Love J C, Wolfe D B, Haasch R, Chabinyc M L, Paul K E, Whitesides G M and Nuzzo R G 2003 *J. Am. Chem. Soc.* **125** 2597
[11] Kondoh H, Iwasaki M, Shimada T, Amemiya K, Yokoyama T and Ohta T 2003 *Phys. Rev. Lett.* **90** 066102
[12] Rufael T S, Huntley D R, Mullins D R and Gland J L 1995 *J. Phys. Chem.* **99** 11472
[13] Baba A, Park M-K, Avincula R C and Knoll W 2002 *Langmuir* **18** 4648
[14] Schweiss R, Werner C and Knoll W 2003 *J. Electroanal. Chem.* **540** 145
[15] Schreiber F 2000 *Prog. Surf. Sci.* **65** 151
[16] Ulman A 1996 *Chem. Rev.* **96** 1533
[17] DeRenzi V, Rousseau R, Marchetto D, Biagi R, Scandolo S and Del Pennino U 2005 *Phys. Rev. Lett.* **95** 046804
[18] Nuzzo R, Zegarski B R and Dubois L H 1987 *J. Am. Chem. Soc.* **109** 733
[19] Fischer D, Curioni A and Andreoni W 2003 *Langmuir* **19** 3567–71
[20] Chidsey C E D and Loiacono D N 1990 *Langmuir* **6** 682
[21] Alexiadis O, Harmandaris V A, Mavrantzas V G and DelleSite L 2007 *J. Phys. Chem.* C at press
[22] Alavi A, Kohanoff J, Parrinello M and Frenkel D 1994 *Phys. Rev. Lett.* **73** 2599
[23] For this work we used the version 3.4 of the CPMD code. Hutter J *et al* 1995–1999 CPMD, copyright MPI für Festkörperforschung and IBM Zurich Research Laboratory
[24] Perdew J P, Burke K and Ernzerhof M 1996 *Phys. Rev. Lett.* **77** 3865
[25] Yourdshahyan Y and Rappe A M 2002 *J. Chem. Phys.* **117** 825
[26] Cometto F P, Paredes-Olivera P, Macagno V A and Patrito E M 2005 *J. Phys. Chem.* B **109** 21737
[27] Akinaga Y, Nakajima T and Hirao K 2001 *J. Chem. Phys.* **114** 8555
[28] Molina L M and Hammer B 2002 *Chem. Phys. Lett.* **360** 64
[29] Gottschalck J and Hammer B 2002 *J. Chem. Phys.* **116** 784
[30] Vargas M C, Giannozzi P, Selloni A and Scoles G 2001 *J. Phys. Chem.* B **105** 9509
[31] Yourdshahyan Y, Zhang H K and Rappe A M 2001 *Phys. Rev.* B **63** 081405(R)
[32] Grönbeck H, Curioni A and Andreoni W 2000 *J. Am. Chem. Soc.* **122** 3839